Bubble dynamics and High Intensity Focused Ultrasound: experimental observations and numerical simulations using Boundary Element Method

[1]Siew-Wan Ohl; [1]Evert Klaseboer; [2]Boo Cheong Khoo*

*[1]Institute of High Performance Computing, A*STAR, Singapore; [2]Dept of Mechanical Engineering, University of Singapore.*

Abstract

We present an experimental study of High Intensity Focused Ultrasound (HIFU) using a parabolic shaped transducer and high speed photography (Ohl et al, 2015). The transducer (Sonic Concept Inc.) has a diameter of 60 mm, and a resonant frequency of 250kHz. When it is driven between 120 to 150 Volt peak-to-peak, concentrated rings of bubbles are formed on top of the transducer. The distance between the rings is about 3 mm, which is half the wavelength of the sound wave produced by the transducer at 250 kHz. The bubbles within the rings are not stable. They move or jump between the rings, or coalesce, or float toward the free surface. To stabilise the rings, we use a reflector which is made of stainless steel, and have the same shape and dimensions as the transducer. At lower driving voltages (80 to 100 Vpp), streams of bubbles are seen moving towards the free surface. This indicates that no standing waves are present. When driven in a burst mode (500 cycles), small bubble clouds are formed. We captured the nucleation and expansion of these clouds using the high speed photography and a long distance microscopic lens. In an attempt to understand some of these observed phenomena, we employed numerical simulations based on the Boundary Element Method (BEM). The Boundary Element Method is an established numerical method for the simulation of bubble dynamics (Blake et al, 1986, 1987). Recently Klaseboer et al (2012) and Sun et al (2014) have improved the numerical solution methodology by eliminating the singularities in the Boundary Integral equation. By using an analytical function, and subtracting this from the original Boundary Integral Method in a specific manner, the method is desingularized, with the added advantage of eliminating the solid angle. This breakthrough significantly reduces the computational complexity and cost, making the use of higher order elements becomes straight forward.The same analytics is applied then to develop a three-dimensional BEM code to solve the Helmholtz equation. The code is used to simulate the ultrasound field generated by the HIFU transducer which is used in the experiments previously mentioned. From the simulation, the focused ultrasound field is clearly described.

Keywords: High Intensity Focused Ultrasound, HIFU, Boundary Element Method, numerical simulation.

1. Introduction

High Intensity Focused Ultrasound was first used in research in the 1930s (Grützmacher, 1936). It is generated typically either with a ceramic or piezo transducer, which has a bowl or a cylindrical shape, or by an array of piezo transducers which are controlled to generate ultrasound with a certain phase differences between them. The HIFU system is able to focus the ultrasound to a certain volume where high pressure or high ultrasound intensity is achieved.

HIFU offer the possibility of non-invasiveness where medical treatments can be administered extra-corporeally. The focus region is heated up, and tissues are lysed or emulsified. This thermal effect is the main mechanism behind the use of HIFU for the treatment of prostate cancer (Poissonnier et al., 2007) and the removal of kidney or liver tumours (Illing et al., 2005). There are new treatments being explored especially in the area of brain surgery, for example to treat essential tremors (Elias et al., 2013).

Another important mechanism offers by HIFU is the generation of cavitation bubbles in the focus region. We have explored using the violently oscillating and collapsing bubbles for the treatment of root canal infection (Shrestha et al., 2009) or the removal or biofilm (Iqbal et al., 2013). These bubbles can be potentially used for localized and timed drug delivery (Dromi et al., 2007), and the non-thermal lysis of tissue via histotripsy (Kim et al., 2014).

Since it is difficult to visualize or tract HIFU generated bubbles in medical treatment, we have attempted to understand the bubble sound waves interaction via experiments and numerical simulations. We will discuss our

*Corresponding Author, Boo Cheong Khoo: mpekbc@nus.edu.sg

experimental observations in the next section. For numerical simulation, we use the Boundary Element Method which is effective and efficient in modeling the change in bubble shapes by allowing meshing only on the bubble surface instead of the whole simulation domain (for example the water tank). From our previous simulations, we found that the bubbles are very sensitive to the intensity and frequency of sound waves (Fong et al., 2008), and also the collapse of the bubbles are dependent on the properties of the nearby tissues (Fong et al., 2006).

2. HIFU Experiments

2.1 Experimental setup

The experimental setup (see Fig. 1(a)) consists of the following items: a custom-made bowl-shaped transducer (Sonic Concept Inc.) which is 60 mm in diameter and has a resonant frequency of 250 kHz; an acrylic tank which is about 20x20x25 cm^3 in dimension; a linear amplifier (AG1021 LF Amplifier/Generator, T&C Power Conversion); and a signal generator (33220A 20 MHz Function/Arbitrary Waveform Generator, Agilent Technologies). The signal generator controls the input signal, which is typically a 5 mV peak-to-peak sinusoidal wave. Its output is channeled into the input of the linear amplifier, which amplifies the voltage to between 80 and 200 Vpp. The linear amplifier is connected to the transducer, which is submerged in the tank, which is filled with tap water. The transducer has been customized to be waterproof.

2.2. Experimental observations

At the resonant frequency of the transducer, i.e. 250 kHz, bubbles are seen to form in the water tank. At high driving voltage (150 to 200 Vpp), rings of bubbles are formed on top of the transducer as seen in Fig. 1(b). The rings can be stabilized with a reflector which is placed on top (below the free surface). The reflector has the same shape and dimensions as the transducer. Note that these rings are observed without the use of the reflector as well. Just that they are less stable and therefore more difficult to image. The wavelength of the standing wave in the tank is calculated as:

$$\lambda = \frac{c}{f}, \qquad (1)$$

where c is the speed of sound in water and f is the frequency of the wave. Given that c is 1500 ms^{-1}, and f is 250 kHz, λ is 0.006 m or 6 mm. The distance between the rings in Fig. 1(b) is about 3 mm. Thus it is verified that the bubbles are trapped at the pressure antinodes of the standing wave. These bubbles are not completely stationary; over time, they coalesce and form bigger bubbles, which will eventually 'escape' from the ring due to buoyancy.

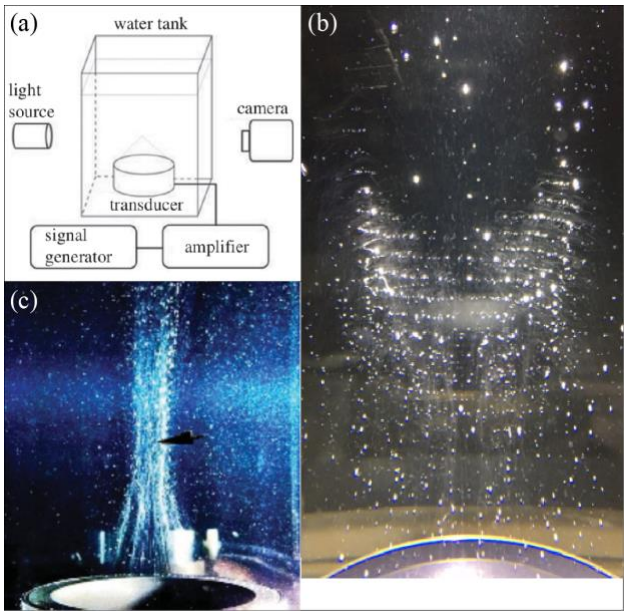

*Corresponding Author, Boo Cheong Khoo: mpekbc@nus.edu.sg

Figure 1 (a) Experimental setup. The transducer is driven by an amplifier, which has an input waveform from the signal generator. The bubbles are generated on top of the transducer in a water tank, and imaging is done with a camera system. (b) Bubble rings on top of the transducer, which is driven at 250 kHz and 200 Vpp. (c) At a lower driving voltage of 80 Vpp, a stream of bubbles is seen to move upwards from the transducer surface.

3. Desingularised Boundary Element Method

The Boundary Element Method is used to solve the potential function that defines the fluid domain. Let us first investigate the more familiar Laplace equation and show the principle of desingularization before moving on to the Helmholtz equation for sound wave simulations in the next section. Interested reader is referred to textbooks on BEM, for example Becker (1992).

We can define a potential $\phi = \phi(\vec{x})$ which satisfies the Laplace equation as:

$$\nabla^2\phi = 0. \quad (2)$$

This equation is equivalent to an equation with only boundary integrals as:

$$c(\vec{x}_0)\phi(\vec{x}_0) + \int_S \phi \frac{\partial G}{\partial n} dS = \int_S G \frac{\partial \phi}{\partial n} dS, \quad (3)$$

where $G = 1/|\vec{x} - \vec{x}_0|$, and it is known as the 3D free space Green function. Equation (3) is referred to as the boundary element (or integral) method. It is noted that both G and $\partial G/\partial n$ are singular with $1/|\vec{x} - \vec{x}_0|$, because $(\vec{x} - \vec{x}_0)$ is perpendicular to the normal vector n when $\vec{x}$ approaches $\vec{x}_0$. In the standard BEM treatment, special quadrature formulae have to be developed for calculations involving the singular integrals

In our desingularized BEM, we choose another known function, say χ, which satisfies the Laplace equation. Then:

$$c(\vec{x}_0)\chi(\vec{x}_0) + \int_S \chi \frac{\partial G}{\partial n} dS = \int_S G \frac{\partial \chi}{\partial n} dS. \quad (4)$$

Also we require the following limits to be satisfied:

$$\lim_{\vec{x}\to\vec{x}_0} \chi(\vec{x}) = \phi(\vec{x}_0), \quad (5)$$

$$\lim_{\vec{x}\to\vec{x}_0} \frac{\partial \chi(\vec{x})}{\partial n} = \frac{\partial \phi(\vec{x}_0)}{\partial n}. \quad (6)$$

Subtracting Equation (4) from Equation (3), the solid angle c is eliminated. Thus

$$\int_S (\phi - \chi) \frac{\partial G}{\partial n} dS = \int_S G \left(\frac{\partial \phi}{\partial n} - \frac{\partial \chi}{\partial n}\right) dS. \quad (7)$$

Equation (7) is a fully desingularized BEM. There are no singularities that require special treatment in the calculation. The only remaining problem is to choose a suitable function χ. One of the possibilities is to use a combination of a constant and a linear function:

$$\chi(\vec{x}) = \phi(\vec{x}_0) + \frac{\partial \phi(\vec{x}_0)}{\partial n} \vec{n}(\vec{x}_0) \cdot (\vec{x} - \vec{x}_0), \quad (8)$$

$$\frac{\partial \chi(\vec{x})}{\partial n} = \vec{n}(\vec{x}) \cdot \nabla\chi(\vec{x}) = \frac{\partial \phi(\vec{x}_0)}{\partial n} \vec{n}(\vec{x}) \cdot \vec{n}(\vec{x}_0). \quad (9)$$

Then Equation (7) becomes:

$$\int_S \left[\phi(\vec{x}) - \phi(\vec{x}_0) - \frac{\partial \phi(\vec{x}_0)}{\partial n}(\vec{x} - \vec{x}_0)\right] \frac{\partial G}{\partial n} dS = \int_S G \left[\frac{\partial \phi(\vec{x})}{\partial n} - \frac{\partial \phi(\vec{x}_0)}{\partial n} \vec{n}(\vec{x}) \cdot \vec{n}(\vec{x}_0)\right] dS. \quad (10)$$

Equation (10) is our desingularized boundary integral method. Interested readers are referred to Klaseboer et al. (2012) for further proof that Equation (7) is indeed non-singular. If the problem under consideration is an external one, then the contribution of the surface at infinity will give an extra term $4 * \pi * \phi(x_0)$ on the left hand side of Equation (10).

3.1 Simulation of HIFU ultrasound field

The desingularized BEM method can be applied to solve the Helmholtz equation as well as presented in Sun et al. (2014). Briefly, the wave equation in the frequency domain is represented as:

$$\nabla^2\phi(\vec{\mathbf{x}}) + k^2\phi(\vec{x}) = 0\,, \quad (11)$$

*Corresponding Author, Boo Cheong Khoo: mpekbc@nus.edu.sg

where k is the wave number. The variable ϕ is now a complex variable. It is clear that if ϕ is a solution, then $\phi e^{i\alpha}$ is also a solution with α as a constant. The corresponding Green function is then $G^k = {e^{ikr}}/{r}$, with $r = |\vec{x} - \vec{x}_0|$. After some manipulation, it is shown in Sun et al. (2014) that one of the possible solutions is:

$$\chi(\vec{x}) = \phi(\vec{x}_0)\cos y + \frac{1}{k}\frac{\partial\phi(\vec{x}_0)}{\partial n}\sin y, \quad (12)$$

with

$$\frac{\partial\chi(\vec{x})}{\partial n} = \left[-k\phi(\vec{x}_0)\sin y + \frac{\partial\phi(\vec{x}_0)}{\partial n}\cos y\right] n(\vec{x}_0)\cdot n(\vec{x}),$$

where

$$y = k\vec{n}(\vec{x}_0)\cdot(\vec{x}-\vec{x}_0).$$

Basically Equation (12) is the solution for two standing waves in which one has nodes and the other antinodes at $\vec{x}_0$. Fig. 2 shows three-dimensional simulation from a fully desingularized Boundary Element Method code. The transducer is bowl-shaped and is vibrating with displacement in the upward and downward directions. The instantaneous potentials of the acoustic field in the surrounding water are shown in Fig. 2(a). High pressure and low pressure regions are clearly seen. In Fig. 2(b) the magnitude of the pressure field is plotted instead. There is a clear region of focus on top of the transducer. Note that in this simulation the transducer is located in an infinite volume of water. There is no reflection from any walls or free surface. Therefore there is no standing wave.

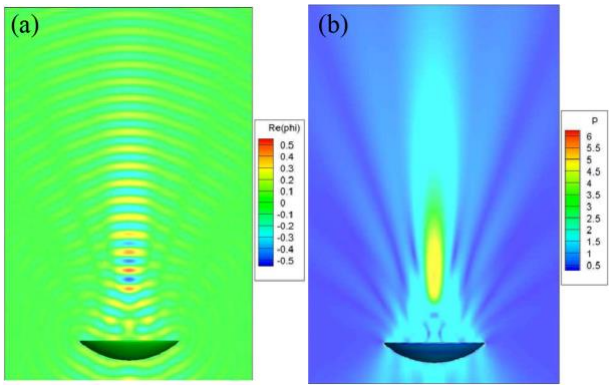

Fig. 2 Three dimensional Boundary Element Method simulation of a wave field in an infinite body of water. (a) The transducer is oscillating up and down. The color code denotes the real part of the instantenous potential in the water. (b) The absolute pressure distribution on top of the transducer is shown. It is noticed that there is a smooth and clear region of focus.

Conclusion

From our HIFU experiment, it is found that HIFU generates cavitation bubbles in its focused region. These bubbles are not stable. They coalesce and move in the sound field. When a standing wave is formed, the bubbles are trapped in the pressure anti-nodes of the sound field. When pulsed ultrasound is used, or when the HIFU is driven with low voltage, the standing wave is not formed and streams of bubbles are seen to travel from the surface of the transducer upwards.

We have also presented a new development in our Boundary Element Method code. A desingularized Boundary Element Method is used to simulate the sound field around a HIFU transducer. It is noted that with the desingularization the complexity in the coding of the Boundary Element Method is greatly reduced because no special treatment is needed for resolving singularities. Also the efficiency of this desingularized method is sufficient to allow the simulation of quadratic elements to solve the Helmholtz equation within a few minutes (for examples see the results in Fig. 2). Thus high resolution and accuracy acoustic simulations can now be done with the desingularized BEM.

*Corresponding Author, Boo Cheong Khoo: mpekbc@nus.edu.sg

Acknowledgement

The authors acknowledge the contributions from the following students from the National University of Singapore in the HIFU experiments: Nigel Chong Jia Wei, and Mohammed Haiqal Haqim Bin Mohd Rahim.

References

Becker, A. A. (1992). The boundary element method in engineering: a complete course. McGraw-Hill Companies.

Blake, J. R., Taib, B. B., & Doherty, G. (1986). Transient cavities near boundaries. Part 1. Rigid boundary. Journal of Fluid Mechanics, 170, 479-497.

Blake, J. R., Taib, B. B., & Doherty, G. (1987). Transient cavities near boundaries Part 2. Free surface. Journal of Fluid Mechanics, 181, 197-212.

Dromi, S., Frenkel, V., Luk, A., Traughber, B., Angstadt, M., Bur, M., ... & Wood, B. J. (2007). Pulsed-high intensity focused ultrasound and low temperature–sensitive liposomes for enhanced targeted drug delivery and antitumor effect. Clinical Cancer Research, 13(9), 2722-2727.

Elias, W. J., Huss, D., Voss, T., Loomba, J., Khaled, M., Zadicario, E., ... & Druzgal, J. (2013). A pilot study of focused ultrasound thalamotomy for essential tremor. New England Journal of Medicine, 369(7), 640-648.

Fong, S. W., Klaseboer, E., Turangan, C. K., Khoo, B. C., & Hung, K. C. (2006). Numerical analysis of a gas bubble near bio-materials in an ultrasound field. Ultrasound in Medicine & Biology, 32(6), 925-942.

Fong, S. W., Klaseboer, E., & Khoo, B. C. (2008). Interaction of microbubbles with high intensity pulsed ultrasound. The Journal of the Acoustical Society of America, 123(3), 1784-1793.

Grützmacher, J. (1936). Ultraakustischer Richtstrahler. *Z. Tech. Phys*, *17*, 166.

Illing, R. O., Kennedy, J. E., Wu, F., Ter Haar, G. R., Protheroe, A. S., Friend, P. J., ... & Middleton, M. R. (2005). The safety and feasibility of extracorporeal high-intensity focused ultrasound (HIFU) for the treatment of liver and kidney tumours in a Western population. British Journal of Cancer, 93(8), 890-895.

Iqbal, K., Ohl, S. W., Khoo, B. C., Neo, J., & Fawzy, A. S. (2013). Effect of high-intensity focused ultrasound on Enterococcus faecalis planktonic suspensions and biofilms. Ultrasound in Medicine & Biology, 39(5), 825-833.

Kim, Y., Hall, T. L., Xu, Z., & Cain, C. A. (2014). Transcranial histotripsy therapy: A feasibility study. IEEE Transactions on Ultrasonics, Ferroelectrics, and Frequency Control, 61(4), 582-593.

Klaseboer, E., Sun, Q., & Chan, D. Y. (2012). Non-singular boundary integral methods for fluid mechanics applications. Journal of Fluid Mechanics, 696, 468-478.

Ohl, S. W., Klaseboer, E., & Khoo, B. C. (2015). Bubbles with shock waves and ultrasound: a review. Interface Focus, 5(5), 20150019.

Poissonnier, L., Chapelon, J. Y., Rouviere, O., Curiel, L., Bouvier, R., Martin, X., ... & Gelet, A. (2007). Control of prostate cancer by transrectal HIFU in 227 patients. European Urology, 51(2), 381-387.

Shrestha, A., Fong, S. W., Khoo, B. C., & Kishen, A. (2009). Delivery of antibacterial nanoparticles into dentinal tubules using high-intensity focused ultrasound. Journal of Endodontics, 35(7), 1028-1033.

Sun, Q., Klaseboer, E., Khoo, B. C., & Chan, D. Y. (2014). A robust and non-singular formulation of the boundary integral method for the potential problem. Engineering Analysis with Boundary Elements, 43, 117-123.

*Corresponding Author, Boo Cheong Khoo: mpekbc@nus.edu.sg